land

MDPI

Article

Analysis of the Spatio-Temporal Patterns of Shrinking Cities in China: Evidence from Nighttime Light

Qi Wang [1], Zhongling Xin [2,3] and Fangqu Niu [2,3,*]

[1] School of Law, Beijing Technology and Business University, Beijing 100048, China; wangq@cupl.edu.cn
[2] Key Laboratory of Regional Sustainable Development Modeling, Institute of Geographic Sciences and Natural Resources Research, Chinese Academy of Sciences, Beijing 100101, China; xinzhongling@126.com
[3] The College of Resources and Environment, University of Chinese Academy of Sciences, Beijing 100049, China
* Correspondence: niufq@lreis.ac.cn

Abstract: Since the 1980s, rapid urbanization in China has been accompanied by city shrinkage. Identifying shrinking cities and clarifying the spatial and temporal patterns are of great significance for formulating policies and realizing smart shrinkage. City shrinkage characterized by population loss is a difficult challenge for urban planning and regional development policy-making. This paper uses 2012–2020 nighttime light (NTL) data to identify the spatial and temporal distribution patterns of shrinking cities in China and excavates the shrinking cities' trend of agglomeration and dispersion further. The following results are obtained. (1) About 34.9% of prefecture-level cities are shrinking across the country but most severely in northeast and northwest China; (2) the number of shrinking cities fluctuates over time (2015 and 2020 are the peak shrinkage years). Shrinking cities in China show a northeast-to-southwest spatial distribution. (3) From 2012 to 2020, the aggregation degree of shrinkage continuously decreased (Low-Low) and the aggregation degree of growth continuously increased (High-High), indicating that shrinkage in northeast China was slightly alleviated and that the radiative effect of the growth pole was further enhanced. These findings help us better understand the trend of city shrinkage in China. Future work needs to be focused on the potential causes of the shrinkage. Furthermore, long-term trends also need to be investigated.

Keywords: shrinking cities; nighttime light data; urban shrinkage intensity; spatial distribution; China

Citation: Wang, Q.; Xin, Z.; Niu, F. Analysis of the Spatio-Temporal Patterns of Shrinking Cities in China: Evidence from Nighttime Light. *Land* **2022**, *11*, 871. https://doi.org/10.3390/land11060871

Academic Editors: Wenze Yue, Yang Chen and Yang Zhang

Received: 9 May 2022
Accepted: 4 June 2022
Published: 8 June 2022

1. Introduction

Shrinking cities originated in the 1970s. Häußermann and Siebel [1] formally proposed the concept of a "shrinking city" in their empirical study of Ruhr, Germany. Based on the life-cycle theory, city shrinkage has been considered as an inevitable stage in the urban development cycle [2]. Characteristics of city shrinkage include an overall decline of the urban center, vacant housing and office buildings, and excess service facilities. On the social level, problems such as rising unemployment and crimes have emerged [3–5]. Since the mid-to-late 20th century, under the combined influence of global economic restructuring, population aging, and suburbanization factors, more western cities have experienced shrinking populations and economic decline. Studies show that more than a quarter of the world's urban population was declining during 1990–2000 [3], and European cities have lost about 40% of their populations [6], especially in former socialist countries of Eastern Europe [7]. Approximately one in ten United States cities in and around the "Rust Belt" are also shrinking [8,9]. In addition, cities in East Asian countries such as South Korea and Japan have shown signs of shrinking to varying degrees [10]. However, studies on shrinking cities have mainly concentrated in Europe and North America [11,12], and little attention is paid to East Asia [13].

Upon developing countries entering the urbanization stage, a large number of people have poured into cities every year and contributed to urbanization. As one of the most

populous developing countries in the world, China's urbanization process has attracted worldwide attention. At the end of the 20th century, Joseph Eugene Stiglitz predicted that there would be two new drivers of global economic development in the 21st century: the new technological revolution led by the United States and China's urbanization. China's urbanization process can be divided into three stages. Before the reform and opening-up stage, China's economic center was spread across heavy industries such as steel, resulting in faster industrialization compared to urbanization. The second stage occurred from 1978 to the end of the 1990s. Small and medium-sized cities achieved a certain degree of development through fewer restrictions on rural migrant workers and the gradual opening of the market economy. The number of small and medium-sized cities has increased rapidly, but their scale has declined significantly. Entering the 21st century, the pattern of urbanization is clear: large, medium, and small cities develop in a coordinated manner with urban agglomerations at the core. Over the past 40 years of reform and opening-up, China has witnessed urbanization at unprecedented rates. Between 1978 and 2019, the urban population increased from 172 million in 1978 to 848 million in 2019; the level of urbanization increased from 17.9% to 60.6% [14].

During this process, growth and expansion are the motivation for urban construction and development. However, problems such as the unrealistically high rate of urbanization and land urbanizing faster than the population have emerged. Catalyzed by globalization and informatization, Chinese cities have entered the era of networks based on flow space. The acceleration of the flow of factors has further triggered the imbalance of competition and cooperation between cities. The population is continuing to gather in major urban agglomerations and megacities. Meanwhile, local shrinkage emerges. Some cities even become "empty cities" or "ghost cities" [15,16]. The phenomenon of shrinkage not only occurs in poorly located areas but also in the "growth pole" of economic development. Wu [17] found that nearly 20 percent of cities/counties/districts of the Beijing-Tianjin-Hebei Region (BTH) and half of the Yangtze River Delta (YRD) exhibit local shrinkage.

The negative change in population is most used to identify city shrinkage [2,18]. Guo and Li [19] used the average population change rate of 5.8% in China as the threshold from 2003 to 2014 to remove the influence of the overall fluctuation on shrinkage identification. Wen et al. [20] set the threshold of the population change rate in China as −0.9% during 2011–2016 based on the natural breakpoint method. Murdoch III [21] determined shrinking cities in the United States by calculating the population loss rate. However, the uniform time interval and shrinking criteria for identifying shrinking cities based on population changes have not yet been established [3,18], and many studies still use zero as a threshold to identify shrinking cities [22]. Increasingly more scholars believe that population loss alone cannot fully capture the characteristics of urban shrinkage [23,24]; they have begun to measure urban shrinkage from multiple dimensions, such as population, economy, and space [25,26]. However, the temporal change of shrinking cities is still rarely considered [18].

China's current research mainly relies on the data of the fifth and sixth population censuses. Long et al. [27] identified 180 cities with varying degrees of shrinkage based on population data at the township and street levels in 2000 and 2010. Zhang et al. [28] used data from two censuses to determine that more than one-third of China's county-level cities have shrunk. However, demographic data often faces problems such as long update cycles, inaccurate statistics, and changes in statistical calibers, etc. Most importantly, China lacks a "city" scope based on functional geographic definitions. The population data obtained by taking administrative boundaries as a statistical unit ignores the inconsistency between urban physical space and the administrative city [29,30], that is, the identification of shrinkage is restricted by the boundaries of administrative divisions.

At present, most studies focus on the urban scale. Due to the lack of statistics that contain micro-spatial information, no distinction is made between a "shrinking city" and "urban shrinkage". According to Haase et al. [4], "shrinking cities" are the cities that have been affected by shrinkage, and "urban shrinkage" is the process of population loss, economic downturn, and related social problems. Spatially, a "shrinking city" is often

viewed as an abstract point, while an "urban shrinkage" focuses on describing the local shrinking process of different areas within the city. In terms of study areas, many studies focus on specific cities [26] and regions [31,32], while national-scale studies are still needed.

At a time when traditional data are inadequate for identifying urban shrinkage, nighttime light data (NTL) provide new methods for research. Studies have proven that there is a significant positive correlation between nighttime light intensity and economic activity intensity; NTL data can be regarded as a comprehensive reflection of changes in urban population, economy, society, and construction [33,34]. With the advantages of high spatial and temporal resolution, high spatial coverage, and no restrictions on administrative regions, NTL has been widely used for extracting urban built-up areas [35,36], the spatialization of social and economic indicators [37], and the reflection of human land-use intensity [38]. NTL data have found early use in identifying urban shrinkage and growth [23,26,31,32]. In studying shrinking cities, NTL can reduce the scope of research to the physical space of the city and describe the internal structure of the city microscopically. This paper uses the National Polar-orbiting Partnership Visible Infrared Imaging Radiometer Suite (NPP-VIIRS) NTL data for 2012–2020 to identify the temporal and spatial distribution patterns of shrinking cities in China.

This study analyzes the regional patterns at a micro level and explores the trends of convergence and dispersion of shrinking cities in China. In this way, the results provide a reference for further research on the phenomenon of urban shrinkage in China and for urban development decision-making.

2. Materials

2.1. Study Area

Without considering the influence of administrative division adjustment factors, this paper uses the Chinese administrative division standard of 2014 to identify shrinking cities. Our study covers 4 municipalities directly led by the nation (MDs), 354 prefecture-level cities (PLCs) in mainland China. The vector data of China's administrative divisions originate from the Resource and Environmental Science Data Center of the Chinese Academy of Sciences (http://www.resdc.cn/, accessed on 8 October 2021).

For region comparisons, we divided the study areas into eight regions [39]: eastern coastal China (ECC), the middle reaches of the Yellow River (MRYLR), the middle reaches of the Yangtze River (MRYTR), northeast China (NEC), northwest China (NWC), northern coastal China (NCC), southern coastal China (SCC), and southwest China (SWC).

2.2. Nighttime Light Data

Two major datasets of global time-series nighttime light data are currently available. One consists of Version 4 series data (1992–2013) derived from the Defense Meteorological Satellite Program's Operational Linescan System (DMSP/OLS), and the other consists of Version 1 series data (2012–present) derived from the Visible Infrared Imaging Radiometer Suite (VIIRS) instrument onboard the Suomi National Polar-orbiting Partnership (NPP) satellite [40]. The data contain a digital number (DN) that indicates the average nighttime light brightness from cities and towns. Although the DMSP data have a longer time span, the DN values (relative brightness) have not been calibrated onboard, thus the DN values at different time periods are not comparable [41]. NPP/VIIRS data are corrected onboard, and the sensor has a higher low-light detection capability and spatial resolution. Gibson et al. [42] pointed out that the VIIRS dataset was a better substitute for economic activity than the widely used DMSP data.

Due to the changing sun angle, parts of northern China have missing imagery in summer [43,44]. To ensure the comparability of the data, this paper uses the more intact monthly (September) data to characterize the light intensity during the year [45]. Accordingly, the dataset used is NPP-VIIRS from 2012 to 2020 for a total of nine periods of data each year.

The NPP-VIIRS dataset is converted into a horizontal axis Mercator (UTM) projection and extracted by superimposing it with the vector data of China. Because the original data only eliminate the effects of noise such as clouds, lightning, and moonlight and does not filter short-term lights such as fires, fishing boat lights, and other temporary light, it is necessary to process abnormally high values of the lighting [46]. Beijing, Shanghai, Guangzhou, and Shenzhen are the most economically developed cities in China. Theoretically, the light intensity across the country should not exceed the highest brightness values in these cities [23]. By analyzing the data, the highest brightness value for each year, the corresponding city (see Table 1), and the data for each year are processed according to (1):

$$DN_{(n,i)} = \begin{cases} DN_{(n,i)} = DN_{(n,max)}, \ DN_{(n,i)} > DN_{(n,max)} \\ DN_{(n,i)} = DN_{(n,i)}, \ 1 \leq DN_{(n,i)} \leq DN_{(n,max)} \end{cases} \quad (1)$$

where n denotes a pixel, i denotes year, and $DN_{(n,i)}$ denotes the digital number of pixel n in year i.

Table 1. Maximum DN values and corresponding cities by year.

Year	$DN_{(n,max)}$	City
2012	337	Beijing
2013	293	Shanghai
2014	308	Beijing
2015	359	Beijing
2016	603	Shanghai
2017	398	Shanghai
2018	470	Shanghai
2019	528	Shanghai
2020	506	Shenzhen

In addition, to eliminate the influence of light changes in the non-urban built-up area on identifying urban shrinkage, we used the threshold method to extract the built-up area. According to existing studies, Ma et al. [47] took 1 nanoWatts/cm^2/sr as the minimum value of an urban stable luminous area. Zhou et al. [23] and Xie et al. [48] assumed that the bright area at night in 2016 covered the bright area prior to 2016 and that the changes in the built-up area from 2016 to 2020 were ignored. Therefore, we extracted the area with DN values greater than 1 nanoWatts/cm^2/sr in the 2016 data for the extent of the built-up area.

3. Methods

First, the shrinking cities were identified based on the continuous NTL data of 358 cities in China. Second, we extract the shrinking areas within the shrinking cities and measure the intensity of urban shrinkage. Finally, we analyze the evolution, convergence, and dispersion trends of shrinking cities in China from temporal and spatial aspects (see Figure 1).

3.1. Identifying Shrinking Cities

Based on the characteristics of the NTL dataset and previous related studies (see Table 2), the criterion to identify shrinkage is proposed.

It is generally accepted that Oswalt and Rieniets [3] set the annual population change rate of less than −1% as the threshold [18]. Thus, we use the TDN change rate of −1% as a threshold. In addition, shrinking research focuses on cities with continuous or frequent shrinking (SCIRN). It is necessary to exclude cities with occasional shrinking. Therefore, shrinkage is defined as continuous (TDN decreased by more than 1% per year for no less than three consecutive years) or frequent (TDN decreased by more than 1% per year over more than one-third of the study period) [49].

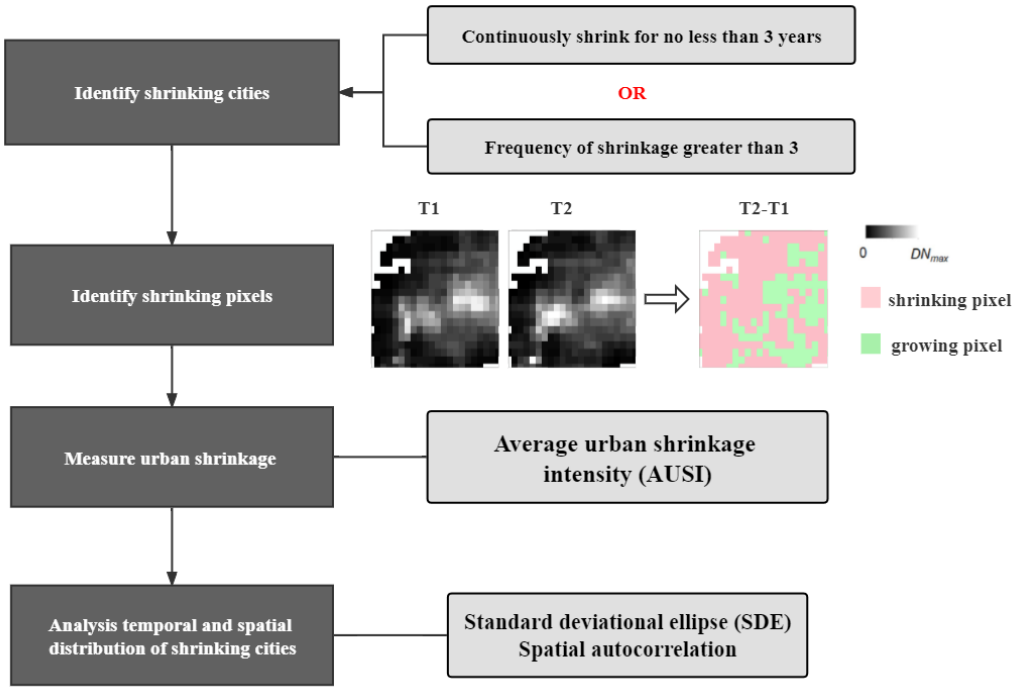

Figure 1. The flowchart for measuring urban shrinkage.

Table 2. Different definitions of shrinking cities put forward by scholars.

Authors	Definitions of Shrinking Cities
Oswalt and Rieniets [3]	Cities where the total population loss is more than 10% or the average annual population loss for three consecutive years is more than 1%.
Shrinking Cities International Research Network (SCIRN) [50,51]	Cities with a population of more than 10,000, experienced two years of population loss.
Wu and Li [52]	Ten years later, the urban population has decreased, and the population growth rate has been negative for more than three natural years.

The specific process is as follows: First, based on the NTL dataset, we calculate the SCII of 358 cities each year from 2012 to 2020 according to (2). Second, if a city has a SCII < −1% for three consecutive years or if the SCII < −1% occurs more than three times, then it is determined to be a shrinking city.

$$SCII_{(n,n+1)}(m) = \frac{TDN_{(n+1)}(m) - TDN_{(n)}(m)}{TDN_{(n)}(m)} \times 100\% \quad (2)$$

where $TDN_{(n)}(m)$ denotes total light intensity of city m in year n.

3.2. Measuring Urban Shrinkage Intensity

With the high spatial resolution of raster images, we can measure the intensity of shrinkage from the perspective of pixel shrinkage. Referring to a previous study, a pixel whose DN decreases by more than 15% in adjacent years is defined as shrinking pixels [49]. The urban shrinkage intensity (USI) is defined as the ratio of the total number of shrinking

pixels to the total number of light pixels of the shrinking city, and the average urban shrinkage intensity (AUSI) is the average of the USI of each year.

$$USI_{(n,n+1)}(m) = \frac{TSP_{n,(n+1)}(m)}{TLP_{(n)}(m)} \times 100\% \quad (3)$$

$$AUSI(m) = \frac{\sum_1^y USI_{(n,n+1)}(m)}{y} \quad (4)$$

where $TSP_{n,(n+1)}(m)$ denotes the total number of shrinking pixels from year n to year $n+1$ in shrinking city m. $TLP_{(n)}(m)$ denotes the total number of light pixels in year n for city m. $AUSI(m)$ is city m's average urban shrinkage intensity, and y is the number of years.

3.3. Spatio-Temporal Evolution Process of Shrinking Cities

3.3.1. Standard Deviational Ellipse (SDE)

To reveal the spatial migration characteristics of shrinking cities in China, the standard deviation ellipse (SDE) algorithm is introduced. SDE is a spatial statistical method that can accurately reveal the characteristics of a spatial distribution [53]. Using the center of gravity, short axis, long axis, and rotation angle as the basic parameters, we calculate the standard deviation of the research object in the X and Y directions to define the axis of the ellipse that contains the distribution of the research object [54].

3.3.2. Spatial Autocorrelation

Studies have shown that shrinking cities are not spatially isolated [18,22]. Spatial autocorrelation analysis can quantify and visualize the clustering of shrinking cities and measure the spatial dependence of research objects. As a spatial autocorrelation index, the global *Moran's I* index can describe the overall distribution of shrinking cities:

$$Moran's\ I = \frac{\sum_{i=1}^n \sum_{j=1}^n W_{ij}(Y_i - \overline{Y})(Y_j - \overline{Y})}{S^2 \sum_{i=1}^n \sum_{j=1}^n W_{ij}} \quad (5)$$

$$S^2 = \frac{1}{n}\sum_{i=1}^n (Y_i - \overline{Y}) \quad (6)$$

$$\overline{Y} = \frac{1}{n}\sum_{i=1}^n Y_i \quad (7)$$

Y_i represents the observation value in the i area, n denotes the number of spatial units, and W_{ij} represents the spatial weight matrix. Global *Moran's I* has the value range [–1, 1]. $I > 0$ indicates that there is a positive spatial correlation between regions. $I < 0$ indicates a negative correlation. $I = 0$ indicates that there is no spatial correlation between regions.

Considering that the global spatial autocorrelation cannot reflect inter-city heterogeneity, local *Moran's I* index is introduced to analyze the clustering characteristics and spatial aggregation patterns of the growth and shrinkage of cities [see (8)]. The local indicators of spatial association (LISA) are used to visualize the patterns. The study period is equally divided into three sections, with 2015 and 2018 as breakpoints to dynamically reveal the spatial convergence and dispersion characteristics of shrinking cities from 2012 to 2020.

$$Local\ Moran's\ I = \frac{Y_i - \overline{Y}}{S^2}\sum_{i=1}^n W_{ij}(Y_i - \overline{Y}) \quad (8)$$

4. Results

4.1. Spatial Distribution and Urban Shrinkage Intensity of Shrinking Cities

Based on the 2016 VIIRS NTL data, the built-up area of China is extracted (see Figure 2). The built-up area is about 47,600 km^2, accounting for about 0.49% of the total area. There is contiguous development of the three major urban agglomerations, the BTH, the YRD,

and the Pearl River Delta (PRD). It is categorized by a disparity in the economic activity intensity between the east and west sides of the Hu line [55].

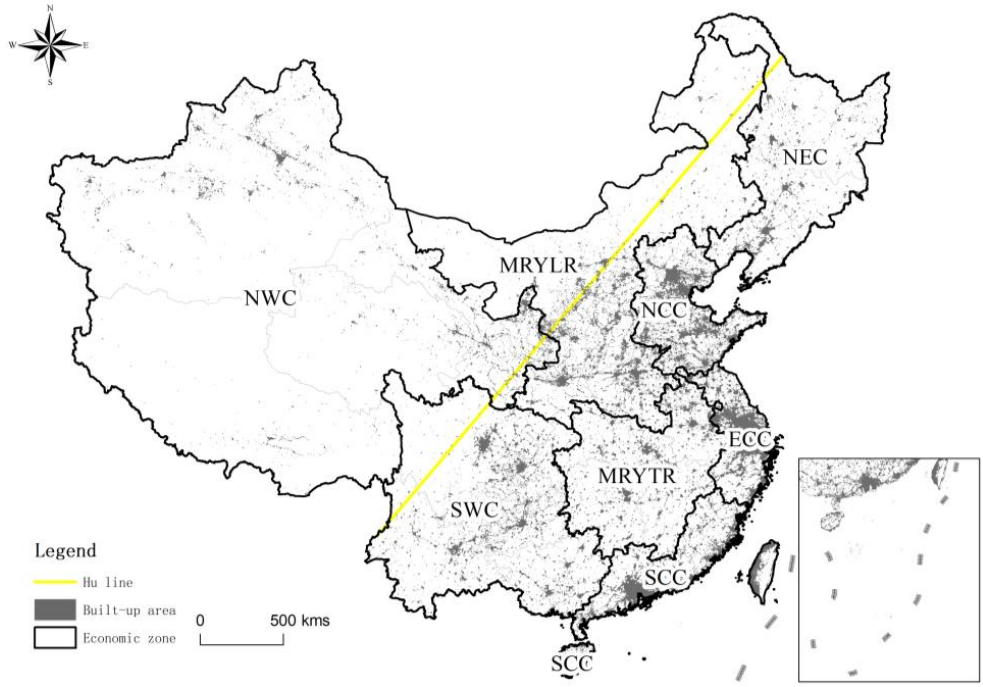

Figure 2. Built-up area of China extracted by VIIRS. (The Hu line in Figure 1 extending from Aihui in the Heilongjiang Province to Tengchong in the Yunnan Province is a demographic demarcation. The southeast, with 36% of the country's area, contains 96% of the Chinese population, while the northwest, with 64% of the total area, contains only 4% [55]. The ratios of populations of the two areas have not changed much despite changes in the national territory and massive urban migration in recent years).

Between 2012 and 2020, shrinking cities were widespread in China, with a total of 125, accounting for 34.9% of all cities (see Figure 3a). In terms of spatial distribution, shrinking cities are scattered all over the country without obvious agglomeration.

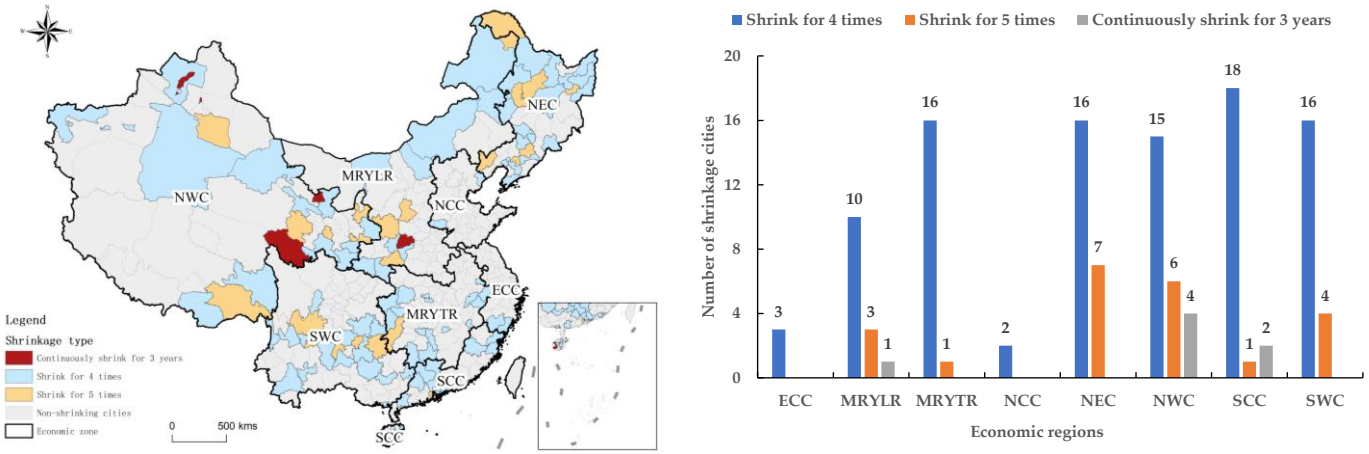

(**a**) (**b**)

Figure 3. (**a**) The spatial distribution of shrinking cities in China, 2012–2020; (**b**) types of shrinking cities in China.

According to the definition of shrinking cities, shrinking cities are divided into two types: "continuously shrinking" and "frequently shrinking". "Continuously shrinking" includes cities that have shrunk continuously for three years, while "frequently shrinking" includes cities that have shrunk up to five times. China's shrinking cities most often shrink four times (76.8% of the total) and five times (17.6% of the total). Of the seven cities that have shrunk for three consecutive years, two are directly administered counties in Hainan Province, while the other five are in the NWC (i.e., Xinjiang, Qinghai, and Yuncheng in Shanxi Province in the MRYLR). Figure 3b shows the statistical results of shrinking cities by economic zone. Regionally, there are 25 shrinking cities in the NWC (20%), followed by 23 in the NEC (18%). The SCC, SWC, MRYLR, and MRYTR values are 21 (17%), 20 (16%), 17 (14%), and 14 (11%), respectively. The regions with the fewest shrinking cities are the NCC and ECC at 2% each. According to the structure and the total number of shrinking cities in the region, shrinking is most severe in the NWC, NEC, and SCC economic regions.

Some of the shrinking cities in the northeast and northwest are resource-exhausted cities. Due to the difficulties of industrial transformation, they have experienced economic decline. They are considered to be typical shrinking cities in China; although they are small in number, their shrinkage is extensive [30]. Cities such as Jixi, Fushun, Qianjiang, and Karamay lost their vitality in regional economic development due to the failure of deindustrialization, resource exhaustion, and low agricultural production efficiency. The result is a decline in local conditions and the gradual flow of skills and technology to the surrounding cities with higher grades. The shrinking cities in the SCC are mainly located in Guangdong and Hainan Provinces. Ledong and Lingshui Autonomous Counties in Hainan have relatively slow economic growth and have not developed in recent years. The distribution of shrinking cities in Guangdong Province shows a clear development gap between cities in northwest Guangdong and the PRD. For the NCC and ECC, there are two major urban agglomerations (BTH and YRD) that act as endogenous drivers of China's economic development, and no shrinkage is identified.

The AUSI of shrinking cities are calculated according to (3) and (4), and classify the cities based on the natural breakpoint method (see Figure 4a). Among the shrinking cities in China from 2012 to 2020, the shrinkage intensity was mainly moderate, and the AUSI was mostly between 15% and 35%. There were 35 (4%), 45 (18%), 46 (46%), 20 (18%), and 7 (11%) cities with low, relatively low, moderate, relatively high, and high USIIs, respectively. Figure 4b is the result of AUSI level statistics by economic region. Cities with severe shrinkage were mainly located in the NEC, NWC, and SWC economic regions.

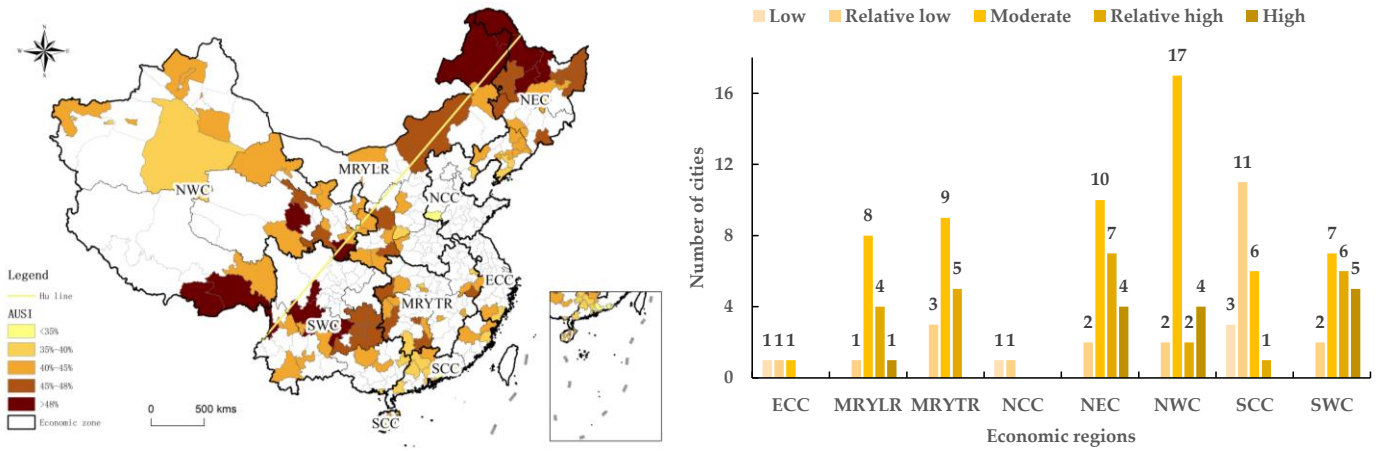

(**a**) (**b**)

Figure 4. (**a**) Spatial pattern of shrinking cities based on AUSI; (**b**) AUSI level statistics by economic regions.

From Figure 4a, we can see that the high and relatively high shrinkage cities are mostly distributed along the Hu Line. Yichun, Hulun Buir, Da Hinggan Ling Prefecture, and Shannan and Nyingchi in Tibet are located in the northwest and southeast of the two endpoints of China. Due to their poor natural environment and marginal economic development, the labor force will inevitably migrate to the surrounding big cities and seek opportunities. In the SWC economic region, Liangshan and Ya'an in the Sichuan Province and Liupanshui and Bijie in the Guizhou Province have helped alleviate poverty for many years. Among them, Liupanshui has faced difficulties in transforming its long-term dependence on the coal industry and has shrunk into a resource-exhausted city. In addition, for the SCC economic region, although the proportion of shrinking cities is higher, the intensity of shrinking is concentrated at a lower level. In fact, there is not a high-shrinkage city, indicating that the shrinkage in SCC is not extensive.

4.2. Spatial-temporal Evolution of Shrinking Cities

This section considers the temporal trend in examining the dynamic changes in shrinkage and growth in China. According to the calculation results of SCII, statistics are conducted by year. $SCII_{(n,n+1)}(m) > 1\%$ is defined as a growing city during the year, $SCII_{(n,n+1)}(m) < -1\%$ is defined as a shrinking city in the current year, and $-1\% < SCII_{(n,n+1)}(m) < 1\%$ is a city with no significant change. From 2012 to 2020, the number of growing and shrinkage periods in China alternate, showing large and irregular fluctuations (see Figure 5). There are two large-scale shrinking events between 2014–2015 and 2019–2020, that is, 2015 and 2020 are the peak years of city shrinkage. It is preliminarily thought that the latest shrinkage is due to the impact of COVID-19. It is not a true "shrinkage", but it also reflects the negative impact of the epidemic on city development.

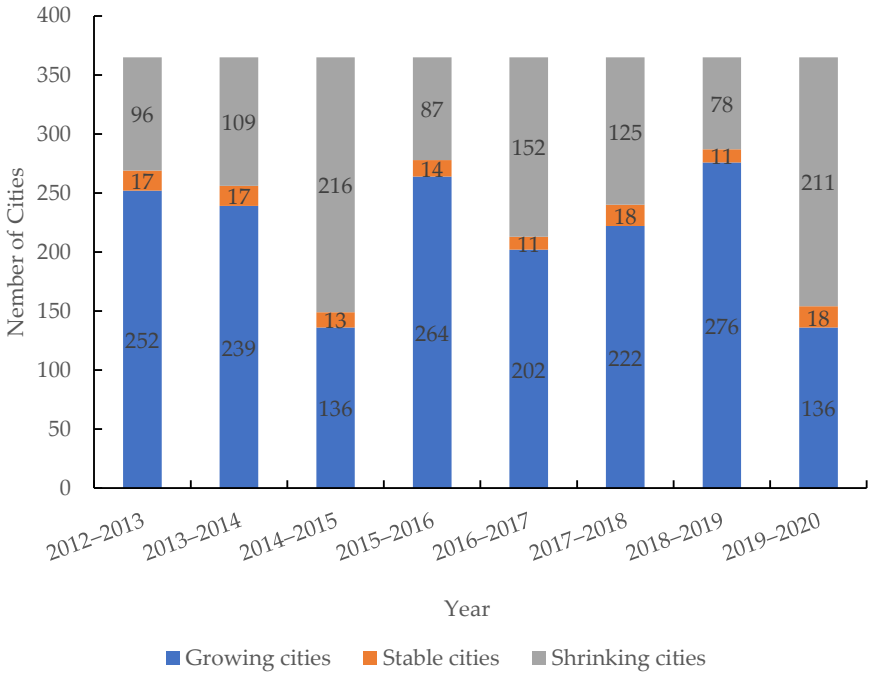

Figure 5. Temporal changes in the number of shrinking cities in China, 2012–2020.

To more intuitively characterize the dynamic migration of shrinking cities in China, the study period is equally divided into three stages: 2012–2014 (stage 1), 2015–2017 (stage 2), and 2018–2020 (stage 3). The directional trends tool in GIS is used to process and obtain the SDEs of the spatial distribution of shrinking cities corresponding to the three stages (see Figure 6). Table 3 shows the parameters of the ellipses.

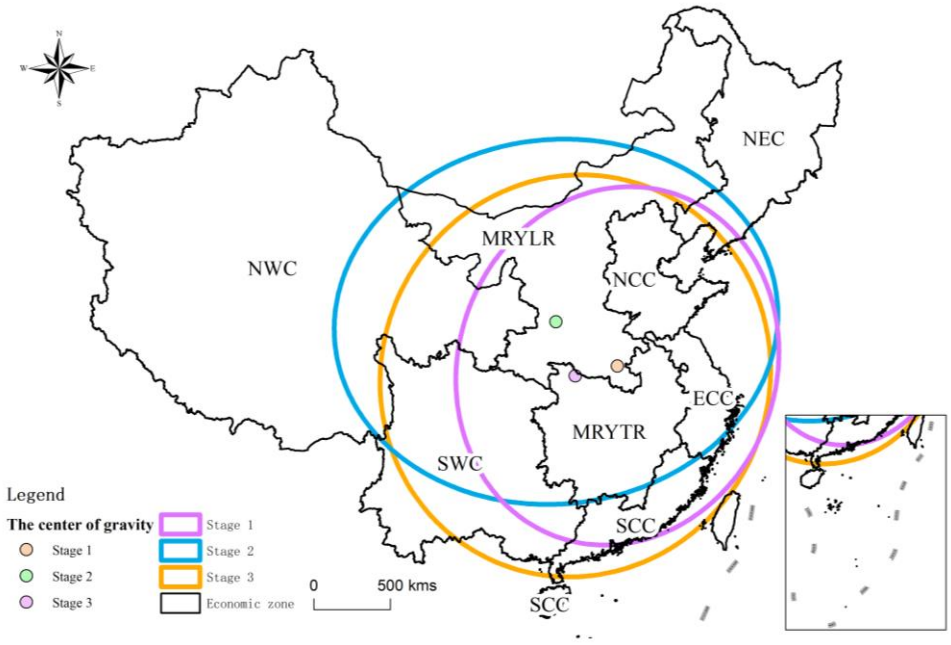

Figure 6. Standard deviation ellipses of urban growth and shrinkage in China from 2012 to 2020.

Table 3. Parameters of SDEs.

Time Span	Area/km^2	Long Axis/km	Short Axis/km	Rotation Angle/Degree
2012–2014	3,880,182	1041	1185	18
2015–2017	5,446,731	4090	3947	84
2018–2020	5,279,090	1269	1323	24

The SDEs of shrinking cities in China from 2012 to 2020 are mainly located in central and eastern China, presenting a "northeast to southwest" spatial distribution. Three ellipse areas show an increasing trend, indicating that the spatial distribution of shrinking cities in China presents spatial decentralization. Among them, the ellipse area of stage 2 increases by 40%, which is consistent with the conclusion that 2015 is the peak shrinkage year. From the perspective of the change trend of the long axis and the short axis, the overall trend is expansion, which also indicates that the spatial layout presents a trend of decentralization. In terms of rotation angle, stage 2 increased significantly, and the ellipse rotated clockwise. The spatial distribution is significant in the east–west direction, which may be due to the shrinkage of the northern cities. The rotation angle of stage 3 is similar to that of stage 1, which may be due to the trend of shrinkage in southwest China or the southern coastal areas; the result is a southward movement of the ellipse. The shrinking center of gravity moved northwest from Zhumadian, Henan Province to Yan'an, Shaanxi Province, and then moved southeast to Shiyan, Hubei Province. In short, the shrinking center of gravity shifted significantly to the northwest and then slightly to the southeast.

4.3. Analysis of Spatial pattern of Shrinking Cities/Growing Cities

The *Moran's I* index of 358 cities in each stage is shown in Table 4, and the significance test *p*-value was 0.00. This passed the significance test at the level of 0.01, which indicates that the spatial distribution of shrinking cities in China is not random; there is a significant positive spatial autocorrelation. Specifically, shrinking cities with similar city shrinkage rates (high-high or low-low) tended to be spatially concentrated. In addition, the *Moran's I* index gradually increases (from 0.049 to 0.183), indicating that cities with similar characteristics continue to cluster.

Table 4. *Moran's I* index during three time periods.

	2012–2014	2015–2017	2018–2020
Moran's I	0.049	0.081	0.183
z-score	7.958	10.091	22.759
p-value	0	0	0

Figure 7a–c display five spatial aggregation patterns in shrinking and non-shrinking cities over three time periods. The high-high (H-H) type represents the aggregation of growing cities, and the low-low (L-L) type represents the aggregation of shrinking cities. The high-low (H-L) type and low-high (L-H) type represent a local aggregation of mixed shrinking and non-shrinking cities. The statistics for the five spatial aggregation patterns in the three time periods are shown in Figure 7d. The number of H-H cities increased steadily, and the number of L-L cities peaked in the second stage but showed an overall decrease. In addition, the global *Moran's I* index shows an increase, indicating that the intensification of agglomeration mainly occurs in the growing cities. In other words, the radiative driving effect of the growth pole is increasing each year, affecting the synchronous development of surrounding cities. For the shrinking cities, the shrinking phenomenon reached the peak in the second stage (consistent with the analysis of SDE), but the spatial agglomeration trend of city shrinkage eased in recent years.

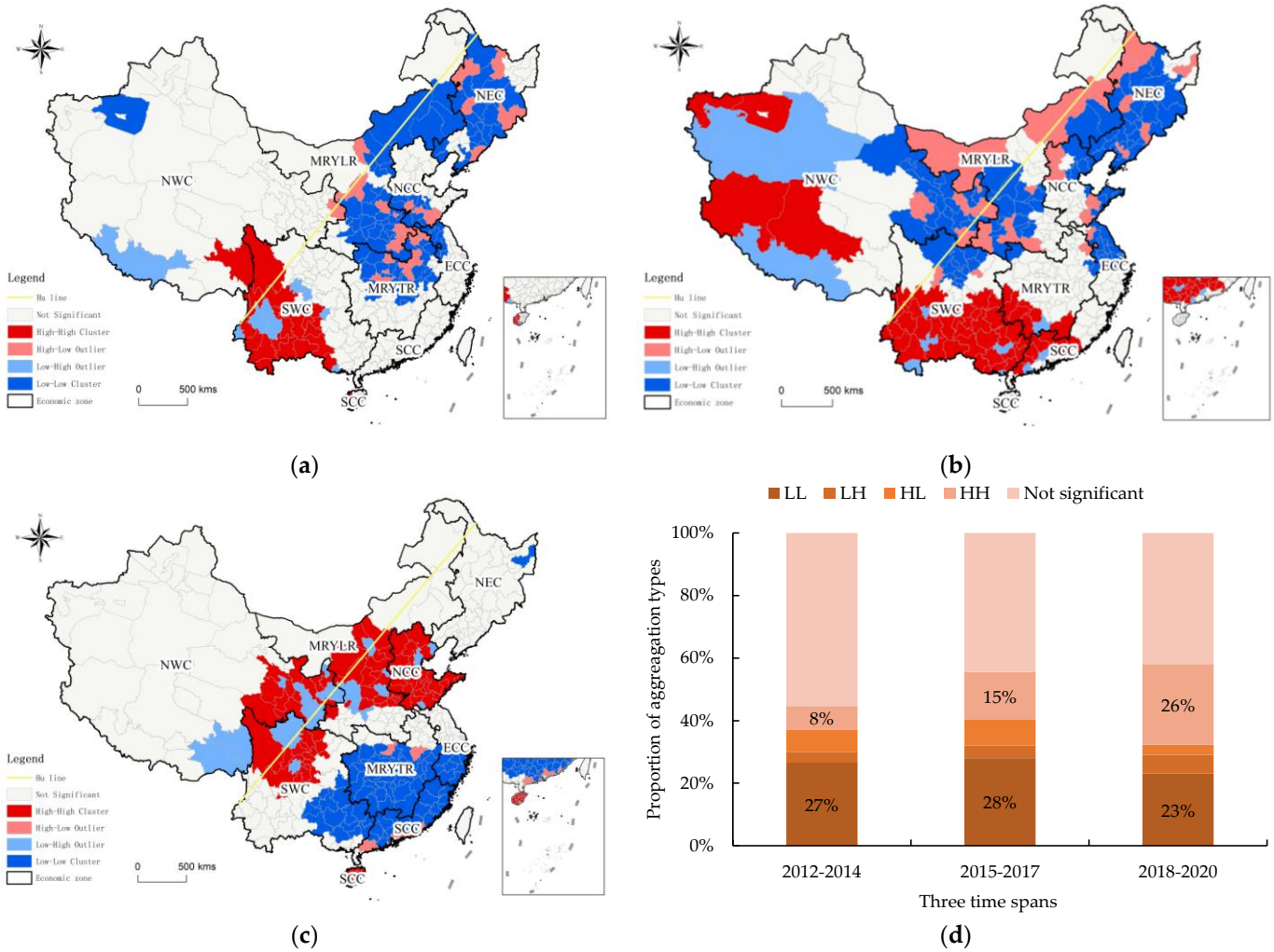

Figure 7. Local *Moran's I* of shrinking cities/growing cities from 2012 to 2020. (**a**) 2012–2014; (**b**) 2015–2017; (**c**) 2018–2020; (**d**) Local *Moran's I* spatial aggregation patterns statistics.

The shrinking hot spots in stage 1 are concentrated in the NEC region, eastern Inner Mongolia, and central cities at the intersection of the MRYLR, MRYTR, NCC, and ECC regions. Subsequently, according to the results of SDE, the shrinkage range in stage 2 expanded and shifted northward (see Figure 7b). L-L cities are mainly distributed in the NEC, the intersection of the NWC and MRYLR, as well as some coastal cities in Hebei, Shandong, and Jiangsu Provinces. The shrinking cities in these areas are mainly resource-based cities and old industrial cities that rely heavily on local resources. By 2018–2020, the L-L clusters moved to the southeast, focusing on the MRYTR, SCC, and partial SWC and ECC (consistent with the results of the shrinkage center of gravity movement trajectory in Figure 6). Under the external impact of COVID-19, coastal areas that are more dependent on exports and investments experienced more severe shrinkage than inland areas. At the same time, China proposed to accelerate the establishment of "a dual circulation" development pattern and focused on the inland economy, moved industries inward, and improved the strategic position of the land border (see Figure 7c).

The growth hot spots in stage 1 are the southwestern part of the SWC region; the main part is the western Sichuan Province and most cities in the Yunnan Province. In 2009, the Central Committee of the Communist Party of China (CPC) put the opening-up of China's border areas and eastern coastal areas on an equal footing, and Yunnan was positioned as "the bridgehead of China's opening-up to the southwest" [56]. In 2010, China regarded accelerating the cultivation of new strategic industries as an important means to promote the upgrading of industrial structure. These may be favorable factors to bring about the urban development of nearly the whole area of the Yunnan Province from 2012 to 2014, as well as from 2015 to 2017. At the same time, cities in southern Xinjiang and western Tibet have also seen a trend of growth. Since the Great Western Expansion campaign in 1999, the state has given increasing policy support to Xinjiang and Tibet. Developed provinces in eastern regions have established a close relationship with these poor cities, assisting in social and economic development, employment promotion, and ethnic unity.

In stage 3, the shrinkage and growth areas have clear directionality, showing a northeast-to-southwest banded distribution that is consistent with the direction of the extension of the Hu line. H-H cities are distributed on both east and west sides of the Hu Line. This pattern indicates that the national development gap has been reduced in recent years, and the BTH region can drive the development of more cities and counties through its strong radiative effect.

5. Discussion

5.1. Validation of Identified Results

China's census data are based on administrative units, so they cannot directly reflect the changes in the urban built-up areas. Only the long-term trends can reflect the shrinking population of cities. Therefore, we calculated the average rate of change of the total population of each prefecture-level city from 2012 to 2020 and extracted cities with an average annual population change rate below 4.7‰ [23]. Figure 8a,b are the shrinking cities identified based on population data and NTL data, respectively. A total of 108 shrinking cities were identified based on population data, which is fewer than the results identified by NTL, and the correlation between the two is low, which is consistent with previous findings [30].

Population loss is only one of the manifestations of urban shrinkage, and there is no specific causal relationship between population changes and urban construction. For example, Luliang in Shanxi Province is facing population decline, but it is still expanding urban space. While in some eastern coastal cities, although the population is increasing, the infrastructure conditions have not changed. Accordingly, the urban environment and urban functional attributes have not improved with population growth. According to Beijing City Lab (BCL), from 2000 to 2010, 8 of the 44 prefecture-level cities that more than quadrupled in urban construction land area saw a decrease in population density (Jiang, et al. [55]). China's urbanization experience is characterized by "focusing on speed but not quality",

which leads to the advance of land urbanization and the dilution of population density [56]. Urban social and economic development is inversely proportional to population, resulting in excessive development, disorderly increase in construction land, and rapid urban space expansion. Eventually, it will exacerbate the phenomenon of urban shrinkage.

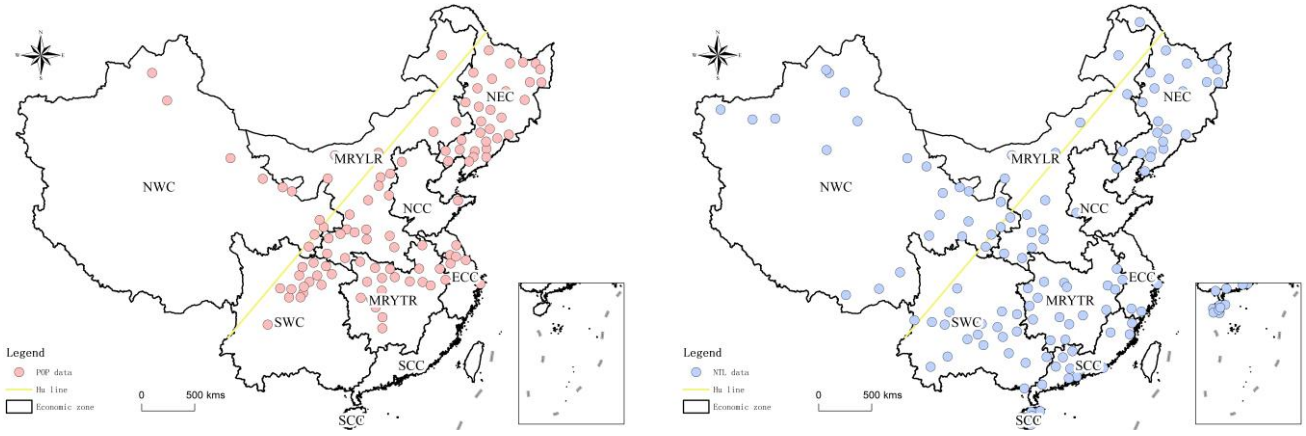

(**a**) (**b**)

Figure 8. (**a**) Shrinking cities identified based on population datasets; (**b**) shrinking cities identified based on NTL.

5.2. Chinese Shrinking Cities Pattern Compared to That of Growing Cities

Based on the analysis in Section 4.3, the growing cities in the first two stages were distributed in the southwest and west, and the third stage moved slightly eastward, showing a northeast–southwest distribution trend along the Hu line.

There is no red zone (H-H) in the eastern coastal urban agglomeration. The reason for this should be that there is large heterogeneity in the development situation in the surrounding geographical area. That is, a small number of cities achieve point-like growth rather than area-like regional growth. Entering the third stage, the radiation-driven effect of the eastern region appears, and the growth regions are distributed across the Hu line, which indirectly shows the trend of the gradual narrowing of the gap between the east and the west.

From the identification results of shrinkage, the northeast of China is the region with the most severe shrinkage, which is consistent with the latest identification results based on the seventh census data [57]. However, from the perspective of the time dimension, the contraction hotspot in the third stage appeared on the southeast coast. Due to negative factors such as COVID-19, the shrinking center of gravity has shifted slightly to the southeast. For example, Dongguan in the PRD, the labeled "world's factory", has lost a significant amount of its population during the industrial transformation period.

5.3. Contributions and Limitations

Compared with traditional data, the NTL dataset in this study is efficient in understanding the trajectories of shrinking cities over a long time period, especially in regions where administrative divisions are frequently adjusted, such as China. Based on the identification, the spatiotemporal patterns and vergence characteristics of urban shrinkage and growth were analyzed, and interesting findings were obtained despite the shorter time scale. Furthermore, the NTL dataset has a global scale, which can provide a global comparative research in the future.

On the other hand, due to the short study period, there may be minor errors in the calibration of the dataset. As remote sensing technology improves, identification and measurement results should be more accurate. Furthermore, the various discriminant methods, evaluating index system, and threshold of shrinkage have not reached a consensus, so more scientific and reasonable criteria need to be considered.

Finally, there are many reasons for cities to shrink. For one, economic factors include the loss of demographic dividends, industrial low costs, and the difficulty of export-oriented manufacturing industry transformation. Moreover, natural factors include extreme weather, frequent natural disasters, and remote mountainous areas. The social and cultural factors include increasing aging and low fertility rates. All these factors may lead to shrinkage. Further empirical research is needed to explore the influencing factors and driving mechanisms of city dynamics.

5.4. Policy Implications

City shrinkage is widespread in China and has become a regular phenomenon. We should accurately understand "shrinkage" from the policy level. Relying on all types of idle land, we should adjust the structure of urban land use and spatial distributions, improve urban infrastructure, and make cities more livable.

5.4.1. Inspirations from EU Shrinking Cities Related Projects

In recent years, the European Union has funded research projects concerning shrinking cities, such as the "Shrink Smart" research project [58] and "Cities Re-growing Smaller" international research network [59]. In practice, several projects related to shrinking cities have also been financed by the European Regional Development Fund of the European Union. These projects include the ALT/BAU Transfer Network, the Re-grow City Transfer Network, 2nd Chance, and Remaking the City [60]. By implementing alternative strategies in European shrinking cities, these projects have activated unused and decaying housing stock resulting from demographic, economic and social change, arrested and reversed long-term social, economic and environmental decline in European shrinking cities. Although China is still in the process of urbanization, the phenomenon of shrinking cities will intensify. Drawing on the European Union's experiences, theoretical and practical research projects on shrinking cities, efficient multi-level governance and policy implementation should be considered.

5.4.2. For the NEC and NWC Economic Regions

Based on the spatial distribution of shrinking cities and urban shrinkage intensity, the NEC and NWC economic regions are the main shrinking regions. Resource-based cities and old industrial cities need to attract talented workers, accelerate industrial transformation and upgrades, and boost the vitality of the economic development. Specifically, (1) increase the proportion of public infrastructure in government fiscal expenditures and focus on the quality of urban construction rather than extensive expansion. (2) Introduce or cultivate local industries, optimize the industrial structure, and increase the diversity of economic activities to address external economic risks.

5.4.3. Playing the Leading Role of Growth Poles in Shrinking Regions

It is worth noting that the contiguous L-L areas in Figure 7 are scattered with H-L type cities. For example, Qingyang in the Gansu Province, Linyi in the Shandong Province, and Songyuan in the Jilin Province are still growing in shrinking hotspots. These cities should be used to foster new growth poles in the region and take advantage of provincial capitals and regional cities in terms of economy, human resources, science, and technology. By virtue of their radiative capacity and attractiveness, these areas will comprehensively promote the coordinated development of other small and medium-sized cities and towns.

6. Conclusions

While China has experienced rapid urbanization, city shrinkage has been widespread. Urban planning has gradually begun to dialectically view city shrinkage and admit the irreversibility of shrinkage, so identifying shrinking cities and clarifying its spatial and temporal patterns is of great significance for formulating policies and realizing smart shrinkage. The purpose of this study is to scientifically understand and evaluate the city

shrinkage in China and to provide a basis for correctly responding to shrinkage. In this paper, we use NTL data to identify shrinking cities in China and analyze their temporal and spatial characteristics. The main findings are as follows:

1. About 34.9% of cities in China have experienced or are experiencing shrinking, which is widely distributed throughout the entire country. The urban shrinkage phenomenon is most severe in northeast and northwest China.
2. Temporally, the number of shrinking cities fluctuates, and 2015 and 2020 are the peak shrinkage years. Spatially, the shrinking cities show a northeast-to-southwest distribution, and spatial dispersion is clear. The shrinking center of gravity moved northwest from Zhumadian, Henan Province to Yan'an, Shaanxi Province, and then moved southeast to Shiyan, Hubei Province.
3. The shrinkage and growth of cities appear to have spatial autocorrelation. The northeast region is the shrinkage hotspot during the first two stages, and the southwest part of SWC is the growth aggregation area. Throughout the entire study period, the aggregation degree of shrinkage continuously decreased (L-L) and the aggregation trend of growth continuously increased (H-H), indicating that the radiative driving effect of the growth pole is further enhanced. The severe shrinkage in the northeast area was slightly alleviated in the late stage. The impact of COVID-19 on areas with export-oriented economies, such as the southeast coast, cannot be ignored.

This study analyzes the spatial and temporal patterns of shrinking cities in China. In the future, it will be necessary to expand the research, including the cyclical theory and potential causes of the shrinkage. Long-term trends need to be investigated by addressing the problem of DMSP and VIIRS integration.

Author Contributions: Conceptualization, Q.W. and F.N.; methodology, Q.W., F.N. and Z.X.; software, F.N. and Z.X.; validation, Q.W. and F.N.; formal analysis, Q.W., F.N. and Z.X.; investigation, Q.W., F.N. and Z.X.; resources, F.N. and Z.X.; data curation, F.N. and Z.X.; writing—original draft preparation, Q.W. and Z.X.; writing—review and editing, Q.W., F.N.; visualization, F.N. and Z.X.; supervision, Q.W., F.N.; project administration, Q.W., F.N.; funding acquisition, Q.W. and F.N. All authors have read and agreed to the published version of the manuscript.

Funding: This research was funded by the National Natural Science Foundation of China, grant number 42071153; the National Social Science Foundation of China, grant number 21ZDA051.

Institutional Review Board Statement: Not applicable.

Informed Consent Statement: Not applicable.

Data Availability Statement: Publicly available datasets were analyzed in this study. A part of the data can be found here: [https://www.ngdc.noaa.gov/eog/dmsp/downloadV4composites.html], accessed 8 October 2021.

Conflicts of Interest: The authors declare no conflict of interest.

References

1. Häußermann, H.; Siebel, W. Die schrumpfende Stadt und die Stadtsoziologie. *Soziologische Stadtforsch.* **1988**, *29*, 78–94. [CrossRef]
2. Alves, D.; Barreira, A.P.; Guimarães, M.H.; Panagopoulos, T. Historical trajectories of currently shrinking Portuguese cities: A typology of urban shrinkage. *Cities* **2016**, *52*, 20–29. [CrossRef]
3. Oswalt, P.; Rieniets, T. *Atlas of Shrinking Cities*; Hatje Cantz: Ostfildern-Ruit, Germany, 2006.
4. Haase, A.; Rink, D.; Grossmann, K.; Bernt, M.; Mykhnenko, V. Conceptualizing urban shrinkage. *Environ. Plan. A* **2014**, *46*, 1519–1534. [CrossRef]
5. Dong, B.; Ye, Y.; You, S.; Zheng, Q.; Huang, L.; Zhu, C.; Tong, C.; Li, S.; Li, Y.; Wang, K. Identifying and classifying shrinking cities using long-term continuous night-time light time series. *Remote Sens.* **2021**, *13*, 31–42.
6. Turok, I.; Mykhnenko, V. The trajectories of European cities, 1960–2005. *Cities* **2007**, *24*, 165–182. [CrossRef]
7. Mykhnenko, V.; Turok, I. East European cities–patterns of growth and decline, 1960–2005. *Int. Plan. Stud.* **2008**, *13*, 311–342. [CrossRef]
8. Schwarz, K.; Berland, A.; Herrmann, D.L. Green, but not just? Rethinking environmental justice indicators in shrinking cities. *Sustain. Cities Soc.* **2018**, *41*, 816–821. [CrossRef]

9. Beauregard, R.A. Urban population loss in historical perspective: United States, 1820–2000. *Environ. Plan. A* **2009**, *41*, 514–528. [CrossRef]
10. Jeon, Y.; Kim, S. Housing abandonment in shrinking cities of East Asia: Case study in Incheon, South Korea. *Urban Studies* **2020**, *57*, 1749–1767. [CrossRef]
11. Audirac, I. Introduction: Shrinking cities from marginal to mainstream: Views from North America and Europe. *Cities* **2018**, *75*, 1–5. [CrossRef]
12. Mallach, A. What we talk about when we talk about shrinking cities: The ambiguity of discourse and policy response in the United States. *Cities* **2017**, *69*, 109–115. [CrossRef]
13. Deng, T.; Wang, D.; Yang, Y.; Yang, H. Shrinking cities in growing China: Did high speed rail further aggravate urban shrinkage? *Cities* **2019**, *86*, 210–219. [CrossRef]
14. National Bureau of Statistics of China. *China Statistical Yearbook*; China Statistics Press: Beijing, China, 2020.
15. Xu, B.; Pang, D. Growth and decline: A study on international urban contraction and its implications for China. *Economist* **2014**, *4*, 5–13.
16. Jin, X.; Long, Y.; Sun, W.; Lu, Y.; Yang, X.; Tang, J. Evaluating cities' vitality and identifying ghost cities in China with emerging geographical data. *Cities* **2017**, *63*, 98–109. [CrossRef]
17. Wu, K. Cognitive misunderstanding and spatial planning response of urban contraction. *Beijing Plan. Rev.* **2019**, *3*, 4–11.
18. Guan, D.; He, X.; Hu, X. Quantitative identification and evolution trend simulation of shrinking cities at the county scale, China. *Sustain. Cities Soc.* **2021**, *65*, 102611. [CrossRef]
19. Guo, Y.; Li, L. Change in the negative externality of the shrinking cities in China. *Sci. Geogr. Sin.* **2019**, *39*, 52–60.
20. Wen, J.; Song, Y.; Ren, G. Assessment of urban contraction in Chin: Based on data from municipal districts at prefecture level and above. *Urban Probl.* **2019**, *9*, 4–10.
21. Murdoch, J., III. Specialized vs. diversified: The role of neighborhood economies in shrinking cities. *Cities* **2018**, *75*, 30–37. [CrossRef]
22. Zhang, Y.; Fu, Y.; Kong, X.; Zhang, F. Prefecture-level city shrinkage on the regional dimension in China: Spatiotemporal change and internal relations. *Sustain. Cities Soc.* **2019**, *47*, 101490. [CrossRef]
23. Zhou, Y.; Li, C.; Zheng, W.; Rong, Y.; Liu, W. Identification of urban shrinkage using NPP-VIIRS nighttime light data at the county level in China. *Cities* **2021**, *118*, 103373. [CrossRef]
24. Bernt, M. The limits of shrinkage: Conceptual pitfalls and alternatives in the discussion of urban population loss. *Int. J. Urban Reg.* **2016**, *40*, 441–450. [CrossRef]
25. Hartt, M. The prevalence of prosperous shrinking cities. *Ann. Assoc. Am. Geogr.* **2019**, *109*, 1651–1670. [CrossRef]
26. Wu, K.; Wang, X. Understanding growth and shrinkage phenomena of industrial and trade cities in southeastern China: Case study of Yiwu. *J. Urban Plan. Dev.* **2020**, *146*, 05020028. [CrossRef]
27. Long, Y.; Wu, K.; Wang, J. Shrinking cities in China. *Modern Urban Res.* **2015**, *9*, 14–19.
28. Zhang, X.; Liu, Y.; Lv, C. The background, identification of shrinking cities in China and characteristic analysis. *Sci. Geogr. Sin.* **2016**, *18*, 132–139.
29. Long, Y. Redefining Chinese city system with emerging new data. *Appl. Geogr.* **2016**, *75*, 36–48. [CrossRef]
30. Jiang, Z.; Zhai, W.; Meng, X.; Long, Y. Identifying shrinking cities with NPP-VIIRS nightlight data in China. *J. Urban Plan Dev.* **2020**, *146*, 04020034. [CrossRef]
31. Niu, W.; Xia, H.; Wang, R.; Pan, L.; Meng, Q.; Qin, Y.; Li, R.; Zhao, X.; Bian, X.; Zhao, W. Research on large-scale urban shrinkage and expansion in the Yellow River affected area using night light data. *ISPRS Int. J. Geo-Inf.* **2021**, *10*, 5. [CrossRef]
32. Chen, T.; Hui, E.C.; Tu, Y.; Lang, W. Growth or shrinkage: Discovering development patterns and planning strategies for cross-border areas in China. *J. Urban Plan. Dev.* **2021**, *147*, 05021046. [CrossRef]
33. Elvidge, C.D.; Hsu, F.-C.; Baugh, K.E.; Ghosh, T. National trends in satellite-observed lighting. *Glob. Urban Monit. Assess. Through Earth Obs.* **2014**, *23*, 97–118.
34. Gennaioli, N.; La Porta, R.; Lopez De Silanes, F.; Shleifer, A. Growth in regions. *J. Econ. Growth* **2014**, *19*, 259–309. [CrossRef]
35. Li, F.; Yan, Q.; Bian, Z.; Liu, B.; Wu, Z. A POI and LST adjusted NTL urban index for urban built-up area extraction. *Sensors* **2020**, *20*, 2918. [CrossRef] [PubMed]
36. Sun, L.; Tang, L.; Shao, G.; Qiu, Q.; Lan, T.; Shao, J. A machine learning-based classification system for urban built-up areas using multiple classifiers and data sources. *Remote Sens.* **2020**, *12*, 91. [CrossRef]
37. Wu, R.; Yang, D.; Dong, J.; Zhang, L.; Xia, F. Regional inequality in China based on NPP-VIIRS night-time light imagery. *Remote Sens.* **2018**, *10*, 240. [CrossRef]
38. Niu, F.; Xin, Z.; Sun, D. Urban land use effects of high-speed railway network in China: A spatial spillover perspective. *Land Use Policy* **2021**, *105*, 105417. [CrossRef]
39. Yang, Y.; He, C.; Zhang, Q.; Han, L.; Du, S. Timely and accurate national-scale mapping of urban land in China using Defense Meteorological Satellite Program's Operational Linescan System nighttime stable light data. *J. Appl. Remote Sens.* **2013**, *7*, 073535. [CrossRef]
40. Li, X.; Zheng, X.; Yuan, T. Knowledge mapping of research results on DMSP/OLS nighttime light data. *J. Geo-Inf. Sci.* **2018**, *20*, 351–359.

41. Elvidge, C.; Ziskin, D.; Baugh, K.; Tuttle, B.; Ghosh, T.; Pack, D.; Erwin, E.; Zhizhin, M. A fifteen-year record of global natural gas flaring derived from satellite data. *Energies* **2009**, *2*, 595–622. [CrossRef]
42. Gibson, J.; Olivia, S.; Boe-Gibson, G.; Li, C. Which night lights data should we use in economics, and where? *J. Dev. Econ.* **2021**, *149*, 102602. [CrossRef]
43. Wu, Y.; Shi, K.; Yv, B.; Li, C. Analysis of the impact of urban sprawl on haze pollution based on the NPP/VIIRS nighttime light remote sensing data. *Geomat. Inf. Sci. Wuhan Univ.* **2021**, *46*, 777–789.
44. Yv, B.; Wang, C.; Gong, W.; Chen, Z.; Shi, K.; Wu, B.; Hong, Y. Nighttime light remote sensing and urban studies: Data, methods, applications and prospects. *J. Remote Sens.* **2021**, *25*, 342–364.
45. Pan, W.; Fu, H.; Zheng, P. Regional poverty and inequality in the Xiamen-Zhangzhou-Quanzhou City Cluster in China based on NPP/VIIRS night-time light imagery. *Sustainability* **2020**, *12*, 2547. [CrossRef]
46. Zhao, J.; Ji, G.; Yue, Y.; Lai, Z.; Chen, Y.; Yang, D.; Yang, X.; Wang, Z. Spatio-temporal dynamics of urban residential CO_2 emissions and their driving forces in China using the integrated two nighttime light datasets. *Appl. Energy* **2019**, *235*, 612–624.
47. Ma, T.; Zhou, C.; Pei, T.; Haynie, S.; Fan, J. Responses of Suomi-NPP VIIRS-derived nighttime lights to socioeconomic activity in China's cities. *Remote Sens. Lett.* **2014**, *5*, 165–174. [CrossRef]
48. Xie, Y.; Weng, Q.; Fu, P. Temporal variations of artificial nighttime lights and their implications for urbanization in the conterminous United States, 2013–2017. *Remote Sens. Environ.* **2019**, *225*, 160–174. [CrossRef]
49. Yang, Y.; Wu, J.; Wang, Y.; Huang, Q.; He, C. Quantifying spatiotemporal patterns of shrinking cities in urbanizing China: A novel approach based on time-series nighttime light data. *Cities* **2021**, *118*, 03346. [CrossRef]
50. Hollander, J. *Polluted and Dangerous: America's Worst Abandoned Properties and What Can Be Done about Them*; University of Vermont Press: Burlington, VT, USA, 2009.
51. Wiechmann, T. Errors expected-aligning urban strategy with demographic uncertainty in shrinking cities. *Int. Plan. Stud.* **2008**, *13*, 431–446. [CrossRef]
52. Wu, K.; Li, Y. Research progress of urban land use and its ecosystem services in the context of urban shrinkage. *J. Nat. Resour.* **2019**, *34*, 1121–1134. [CrossRef]
53. Wong, D.W. Several fundamentals in implementing spatial statistics in GIS: Using centrographic measures as examples. *Geogr. Inf. Sci.* **1999**, *5*, 163–174.
54. Zhao, L.; Zhao, Z. Projecting the spatial variation of economic based on the specific ellipses in China. *Sci. Geol. Sin.* **2014**, *34*, 979–986.
55. Hu, H. The distribution of population in China, with statistics and maps. *Acta Geogr. Sin.* **1935**, *2*, 33–74.
56. General Office of the State Council. Opinions of The State Council on supporting Yunnan Province to Accelerate the Construction of Important Bridgeheads Opening to the Southwest. 3 November 2011. Available online: www.gov.cn/zwgk/2011-11/03/content_1985444.htm (accessed on 20 January 2022).
57. Meng, X.; Long, Y. Shrinking cities in China: Evidence from the latest two population censuses 2010–2020. *Environ. Plan. A Econ. Space* **2022**, *54*, 449–453. [CrossRef]
58. Rink, D.; Haase, A.; Bernt, M.; Großmann, K. *Addressing Urban Shrinkage Across Europe–Challenges and Prospects*; Shrink Smart Research Brief No. 1; Shrink Smart: Leipzig, Germany, 2010.
59. Großmann, K.; Bontje, M.; Haase, A.; Mykhnenko, V. Shrinking cities: Notes for the further research agenda. *Cities* **2013**, *35*, 221–225. [CrossRef]
60. Aurambout, J.P.; Schiavina, M.; Melchiori, M.; Fioretti, C.; Guzzo, F.; Vandecasteele, I.; Proietti, P.; Kavalov, B.; Panella, F.; Koukoufikis, G. *Shrinking Cities*; JRC126011; European Commission: Brussels, Belgium, 2021.